



Science Arts & Métiers (SAM)

is an open access repository that collects the work of Arts et Métiers Institute of Technology researchers and makes it freely available over the web where possible.

This is an author-deposited version published in: <https://sam.ensam.eu>
Handle ID: <http://hdl.handle.net/10985/25561>

To cite this version :

Ghazala SHAFIQUE, Francois GRUSON, Frédéric COLAS, Xavier GUILLAUD - Behaviour of Modular Multilevel DC/DC Converter With DC Voltage Control Integrated in a Multi-terminal DC System Under Fault Conditions - In: 13th International Conference on Power Electronics, Machines and Drives (PEMD 2024), France, 2024-06 - Proceedings of the 13th International Conference on Power Electronics, Machines and Drives (PEMD) - 2024

Any correspondence concerning this service should be sent to the repository

Administrator : scienceouverte@ensam.eu



Behaviour of Modular Multilevel DC/DC Converter With DC Voltage Control Integrated in a Multi-terminal DC System Under Fault Conditions

Ghazala Shafique, François Gruson, Frederic Colas, Xavier Guillaud

Univ. Lille, Arts et Métiers Institute of Technology, Centrale Lille, Junia, ULR 2697 - L2EP - Laboratoire d'Électrotechnique et d'Électronique de Puissance, F-59000 Lille, France

**E-mail: ghazala.shafique@ensam.eu*

Keywords: DC/DC CONVERTER, DC FAULT PROTECTION, DC VOLTAGE CONTROL, FRONT-TO-FRONT MODULAR MULTILEVEL CONVERTER (F2F-MMC), MULTI-TERMINAL HVDC GRIDS

Abstract

The development of multi-terminal DC (MTDC) networks has various challenges as interconnecting grids of different voltages and grounding schemes, DC grid protection and power flow. DC/DC converter has emerged as the solution for interconnecting HVDC links with different specifications. In this paper, the Front-to-Front Modular Multilevel Converter (F2F-MMC) topology is adopted for DC/DC converter, which can act as a firewall between the healthy and faulty grid during DC faults. Along with this, DC/DC converters when operated in DC voltage control mode can provide supplementary functionalities such as participating in DC grid voltage management and increasing the reliability of the system. In this study, the F2F-MMC converter is operated with a virtual resistance DC voltage controller integrated into an MTDC system. A pole-to-pole DC fault is applied on the MTDC grid and the influence of the virtual resistance controller associated with the DC/DC converter is studied for re-establishing the power flow after DC faults.

1 Introduction

High voltage (HV) DC transmission has emerged to be more beneficial than HVAC for long distance power transmission due to good economical factors and low losses. Most of the existing HVDC systems are point-to-point (P2P) links connecting two stations. To have a more reliable and flexible HVDC system, Multi-terminal DC (MTDC) networks are being focussed, as interconnecting several MTDC networks would eventually emerge the concept of DC supergrid [1, 2]. In the future, building an MTDC system would require interconnecting existing P2P links with different specifications such as different voltage levels, grounding topologies (monopolar, bipolar) and HVDC converter technology (voltage source converter or line commutated converters). Thus, in order to adapt these differences, DC/DC converters play an important role as the mandatory intermediate component [3–5]. Various topologies of DC/DC converter have been presented in the literature for HVDC application [6, 7]. An attractive and widely known topology based on a modular multilevel converter (MMC) structure is the Front-to-Front MMC (F2F-MMC) converter providing galvanic isolation [8].

One of the major challenges of an HVDC system is the protection and system behaviour during DC faults. Over the past years, the studies on the integration of DC/DC converter in an MTDC system have increased. Various studies have been carried out to discuss the role of DC/DC converters in protection strategies stopping the fault propagation to the healthy side of the MTDC grid [8–11]. However, in these studies, the DC/DC converter is considered to work with constant power and its power flow is not changed upon the DC faults. No studies have

discussed the situation where a DC/DC converter is operated in voltage control mode and the power flow is changed to restore the remaining system after the occurrence of a DC fault.

An important aspect of HVDC system is to have a robust DC voltage management system. There are various DC voltage controllers known, associated with AC/DC converters but not linked to DC/DC converters in an HVDC system. DC/DC converters can provide additional services as they are highly controllable devices [5, 12]. Thus, a DC voltage controller associated with a DC/DC converter has been proposed named, virtual resistance DC voltage control, to provide support to the DC voltage management system of both interconnected grids. This controller behaviour has been validated through electromagnetic transient (EMT) simulation of a test MTDC system in normal operating conditions with small disturbances.

In this paper, the research has been extended to study the influence of a DC/DC converter with the virtual resistance voltage controller on the system dynamics for re-establishing the power flow after a DC fault. An EMT study has been made on an MTDC system with two P2P links of different specifications interconnected with a modular multilevel DC/DC converter (F2F-MMC). The DC/DC converter is operated in voltage control mode with the virtual resistance DC voltage controller. The simulations are carried out in Matlab/Simulink and a worst-case of pole-to-pole DC faults is applied on the proposed MTDC system. The impact of the DC/DC converter operating with the DC voltage controller has been analysed on the restoration of the MTDC system. Two cases are considered, where in the first case, F2F-MMC is blocked during the fault in order to protect the healthy grid. Whereas, in the second case, instead of blocking, a control scheme is applied to

the F2F-MMC converter to stop the propagation of faults to the healthy side and to have a smoother transition of DC/DC converter power.

The rest of the paper is as follows. Section 2 presents the virtual resistance DC voltage controller associated with the DC/DC converter. Section 3 briefly presents the modelling and control methodology adopted for the MTDC system and its behaviour in normal operating conditions. Section 4 highlights the impact of the virtual resistance controller on the restoration of the MTDC system in critical cases of DC faults.

2 Virtual resistance DC voltage control with DC/DC converter

2.1 Structure of test MTDC system

The studied MTDC system integrating DC/DC converter is presented in Fig 1. It consists of two point-to-point HVDC grids with different voltage levels interconnected through F2F-MMC DC/DC converter. Each DC grid is based on MMC HVDC technology and has a symmetric monopole configuration. The AC grids at each station are modelled with an ideal voltage source with a series impedance. The circuit breakers (CB) are modelled as an ideal switch and the DC cables used are modelled using frequency dependent PI-model proposed by [13].

DC grid 1 is a $\pm 320kV$ network, where MMC11 is in voltage droop control mode with droop coefficient k_{dr1} and MMC12 in power control mode. Similarly, DC grid 2 is a $\pm 250kV$ network with two stations MMC21 (voltage droop control mode with droop coefficient k_{dr2}) and MMC22 (power control mode). The F2F-MMC converter interconnects the two grids at the middle of the respective DC cables.

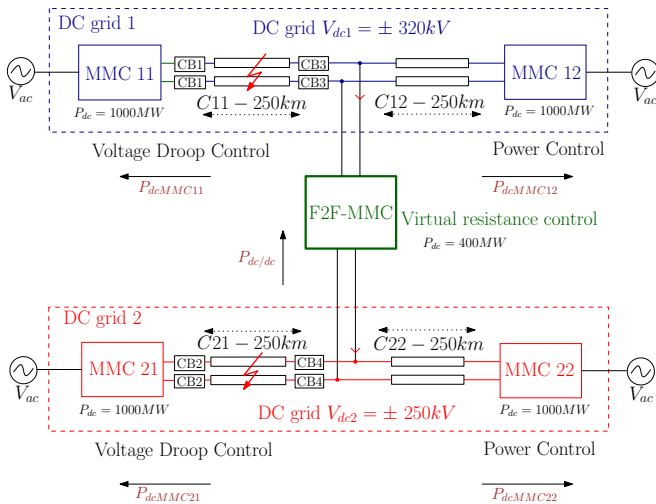


Fig. 1: Case study MTDC system layout

2.2 Principle of virtual resistance DC voltage controller

In addition to exchanging a desired constant power between the interconnected systems, the DC/DC converter can help establish a link between the interconnected HVDC systems. Such that, both networks can provide DC voltage support to each other in case of power disturbance. Thus, the reference power of DC/DC converter $P_{ref}^{dc/dc}$ is given by equation (1), where $P_o^{dc/dc}$ is the constant nominal power (TSO reference) and the additional power $\Delta P^{dc/dc}$ is associated to virtual resistance DC voltage controller for providing DC voltage support.

$$P_{ref}^{dc/dc} = P_o^{dc/dc} + \Delta P^{dc/dc} \quad (1)$$

The virtual resistance DC voltage controller principle is inspired by the well-known DC voltage droop control methodology. The controller acts as virtual resistance linking different HVDC networks. The main objective is to control and provide support to the DC voltages of the MTDC grids interconnected through DC/DC converter. Virtual resistance control structure is presented in Fig 2 and the relation is given by equation (2), where the variables V_{dc1} , V_{dc2} are the measured DC grid voltages, ntr is the rated DC voltage ratio (V_{dc2}/V_{dc1}) and R_{dr} is the resistance droop coefficient.

$$\Delta I^{dc/dc} = (-1/R_{dr})(V_{dc2} - ntrV_{dc1}) \quad (2)$$

Due to any disturbance in the MTDC system, if the DC grid voltages deviate from their rated value, the virtual resistance controller acts and generates the compensating current $\Delta I^{dc/dc}$ depending on the deviated DC voltages and resistance droop coefficient, in order to balance the power among MTDC grids. The corresponding compensating power reference $\Delta P^{dc/dc}$ is derived as in equation (3).

$$\Delta P^{dc/dc} = (-1/R_{dr})(V_{dc2}^2 - ntrV_{dc1}V_{dc2}) \quad (3)$$

The resistance droop coefficient R_{dr} is designed using the relation in equation (3), considering the steady state constraints on the power variation $\Delta P^{dc/dc}$ and the maximum deviation of the DC grids voltages V_{dc2} and V_{dc1} depending on their respective voltage droop controller coefficients. Thus, the virtual resistance controller enables coupling between interconnected grids for sharing the power disturbance and managing the DC grid voltages, as a result reducing the stress on the DC voltage management system.

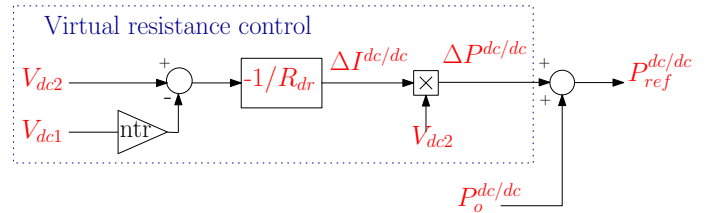


Fig. 2: Virtual resistance DC voltage controller schematic

3 Modelling, control and dynamic behaviour of MTDC system

This section presents the modelling and control approach adopted for MMCs and DC/DC converters. In the later part, the dynamic behaviour of the test system integrating the virtual resistance DC voltage controller is presented under normal operation.

3.1 Modeling and control of MMC and F2F-MMC converter

3.1.1 Modeling and control of MMC: All MMC are modelled with an average arm model including the block state of the converter shown in Fig 3 [14, 15]. Half Bridge sub-module (HBSM) topology is considered in order to have low losses and cost. The average arm model is realised assuming that the voltages across the SMs capacitor are well balanced, i.e., the low-level control is well achieved. The voltage generated by inserted SMs per arm is represented by a controlled voltage source. An equivalent capacitor C_{eq} with a voltage $V_{C_{totu,l}}$ represents the capacitive storage part of the arm with a controlled current source representing the charge/discharge of the capacitor.

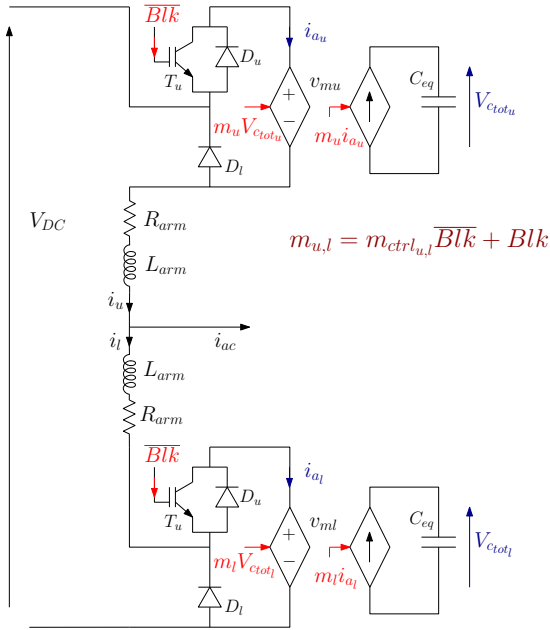


Fig. 3: MMC arm block model

The block state of the converter is the state in which within an SM, both transistors are turned off, generally used in case of analyzing DC faults. Block state is realised, adding an IGBT (T_u, D_u) and an antiparallel diode (D_l) [14]. During the normal operation ($Blk = 0$), T_u is turned ON and the arm current ($i_{u,l}$) flows through the controlled voltage source charging or discharging the equivalent capacitor. The modulation ratio ($m_{u,l}$) is equal to $m_{ctrl_{u,l}}$, which is the value related to the MMC converter control. On the other hand, during the blocked state ($Blk = 1$), transistor T_u is turned OFF and the arm current

flows through either D_u or D_l depending on the current polarity. Here, the equivalent capacitor voltage remains constant. The modulation ratio $m_{u,l} = 1$, so the arm voltage is equal to the sum of all SM capacitor voltage.

The dynamics of the MMC average arm model is represented by equation below [16]. The MMC arm currents are decoupled in AC and DC components. The DC component current (differential current) dynamics is represented by equation (4) and the AC current is given by equation (5) in dq frame. The upper and lower arm equivalent capacitor stored energy is given by equation (6). The stored energies are decoupled using the sum and difference energy and its dynamics are presented in equation (7).

$$\frac{v_{dc}}{2} - v_{diffj} = L_{arm} \frac{di_{diffj}}{dt} + R_{arm} i_{diffj} \quad \text{where,} \quad (4)$$

$$i_{diffj} = \frac{i_{uj} + i_{lj}}{2}, v_{diffj} = \frac{v_{mu_j} + v_{ml_j}}{2}$$

$$\begin{aligned} v_{vd} - v_{gd} &= L_{AC} \frac{di_{gd}}{dt} + R_{AC} i_{gd} + L_{AC} \omega i_{gq} \\ v_{vq} - v_{gq} &= L_{AC} \frac{di_{gq}}{dt} + R_{AC} i_{gq} - L_{AC} \omega i_{gd} \end{aligned} \quad \text{where,} \quad (5)$$

$$\begin{aligned} R_{AC} &= R_g + \frac{R_{arm}}{2}, L_{AC} = L_g + \frac{L_{arm}}{2} \\ \text{and } v_{vj} &= \frac{-v_{mu_j} + v_{ml_j}}{2} \end{aligned}$$

$$\frac{C_{eq}}{2} \frac{dv_{C_{totu_j}}^2}{dt} = \frac{dW_{uj}}{dt}, \quad \frac{C_{eq}}{2} \frac{dv_{C_{totl_j}}^2}{dt} = \frac{dW_{lj}}{dt} \quad (6)$$

$$\begin{aligned} \left\langle \frac{dW_{uj}}{dt} + \frac{dW_{lj}}{dt} \right\rangle_T &= \left\langle \frac{dW_j^\Sigma}{dt} \right\rangle_T = v_{dc} I_{diffj-DC} - P_{ACj} \\ \left\langle \frac{dW_{uj}}{dt} - \frac{dW_{lj}}{dt} \right\rangle_T &= \left\langle \frac{dW_j^\Delta}{dt} \right\rangle_T = -2V_{gj} I_{diffj-AC} \cos \delta \end{aligned} \quad (7)$$

The control structure of MMC is shown in Fig 4, designed based on the inversion based rule. It consists of controlling arm currents and equivalent capacitor voltages. The control approach discussed in [16] is adopted, including balancing of differential currents to eliminate the perturbations in DC current [17]. The equivalent capacitor voltages $V_{C_{totu,l}}$ is controlled by controlling its equivalent stored energy. The control of arm currents are achieved by controlling its decoupled AC and DC components.

3.1.2 Modeling and control of F2F-MMC: The F2F-MMC structure is similar to cascading two MMC front to front and interconnecting AC sides with a transformer as shown in Fig 5. F2F-MMC is modelled using the average arm model of the

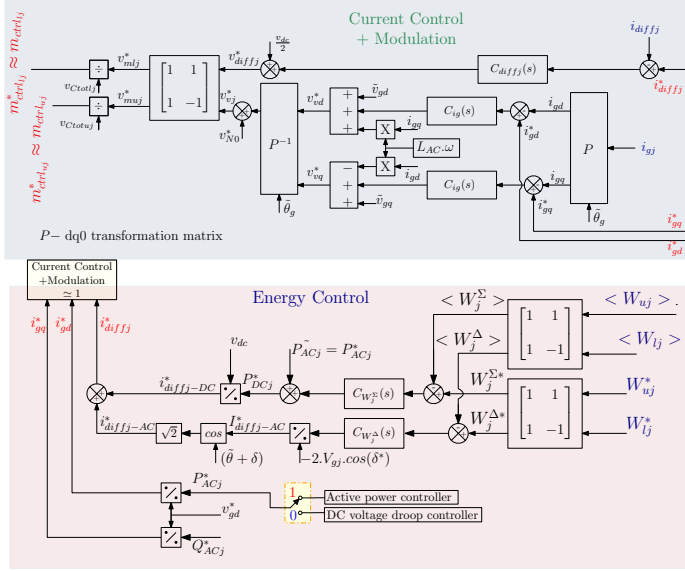


Fig. 4: MMC control structure

MMC with block state as discussed in previous section. Also, the differential current and stored energy controllers of both side MMC are similar to the control discussed previously. Since the AC part of both sides is coupled with a transformer, we adopt the control approach presented in [8]. Here, the primary side MMC fixes its AC voltage to the value $v_{dc1/2}$ and the secondary side MMC controls the AC current in dq frame. The power reference to control the AC current is given by virtual resistance DC voltage control as F2F-MMC works in voltage control mode.

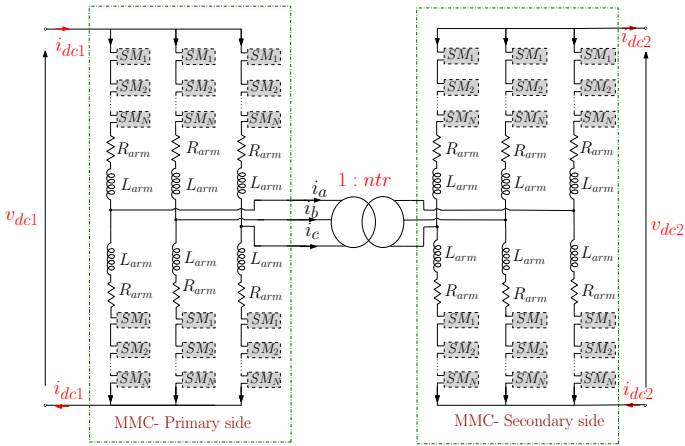


Fig. 5: F2F-MMC Topology

3.2 Behaviour of MTDC system under normal operation

In this section, the dynamic behaviour of the MTDC system (Fig 1) integrating F2F-MMC with the virtual resistance controller is presented in case of power disturbances at the DC grids. The system parameters are given in Table I.

Table 1 System parameters

Parameter	Values
v_{dc1}	640kV
v_{dc2}	500kV
Voltage ratio $1/ntr$	1.28
Length of DC grid 1	500km
Length of DC grid 2	500km
k_{dr1}	0.05p.u.
k_{dr2}	0.05p.u.
$P_{rated}^{dc/dc}$	$\pm 400MW$
R_{dr}	8.0833 Ω
AC voltage V_{ac}	320kV

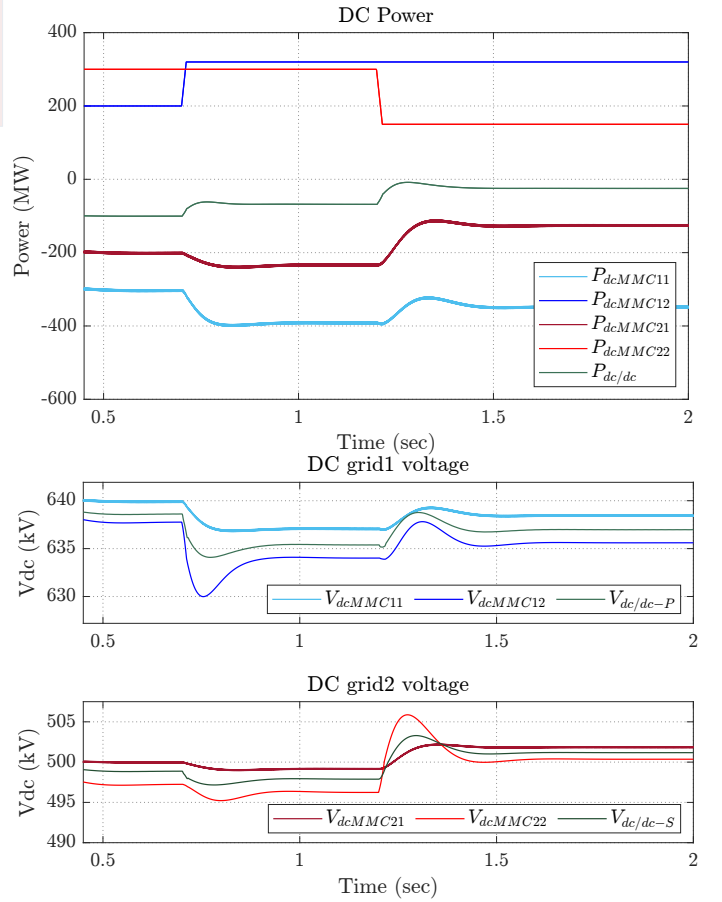


Fig. 6: Normal operation: Variation of DC power (at MMC11, MMC12, MMC21, MMC22, F2F-MMC) and DC grid voltages

At $t = 0.7sec$, a power disturbance is introduced in DC grid 1 at station MMC12, increasing the power by 120MW(0.12p.u.). The resulting DC grid voltages and DC powers at all stations are presented in Fig 6. As a result of power disturbance, the DC grid 1 voltage starts to decrease, thereby activating the virtual resistance controller. So, the power imbalance at DC grid 1 is compensated by voltage droop controlled station MMC11 (DC grid 1) as well as voltage controlled station MMC21 at DC grid 2. Thereby, sharing the

power disturbance between the two grids and maintaining DC voltages under the specified limits (5% usually).

Similarly, at $t = 1.2\text{sec}$, the power at station MMC22 of DC grid 2 is decreased by $150\text{MW}(0.1p.u.)$. As we can observe from Fig 6, this power disturbance at DC grid 2 is compensated by voltage controlled station MMC11 and MMC21 of both DC grids. Therefore, through the virtual resistance controller, we are able to share the power disturbance and manage the DC voltages of both sides of MTDC system, thus, increasing the reliability of the system.

4 Impact of virtual resistance DC voltage controller on the restoration of MTDC system under faulty conditions

When a DC fault occurs at DC grid1 (or DC grid2) at cable C12 (or C22), i.e near a power controlled station MMC12 (or MMC22), then F2F-MMC due to its fault blocking capability can stop the propagation of the fault. The fault and station MMC12 (or MMC2) can be isolated by opening the circuit breakers. With the remaining system, the power flow can be re-establish accordingly as MMC11 (or MMC21) is a voltage control station and can modify its power to compensate the loss of MMC12 (or MMC22) station. Thus, this case is not the critical case to study.

Whereas, if a DC fault occurs at cable C11 (or C21) and isolating the fault will result in loss of a voltage control station MMC11 (or MMC21), then the whole DC grid 1 (or DC grid 2) will collapse. Therefore, this is the most significant case to analyse and restore the faulty grid. In this section, the influence of the virtual resistance controller integrated with the DC/DC converter is studied on the restoration of the MTDC system under such critical cases of DC faults.

4.1 Case 1: Pole-to-pole fault at DC grid1 with blocking mode of F2F-MMC

At 0.8sec a pole-to-pole fault is applied at the middle of cable C11, i.e., at 125km from station MMC11. The resulting behaviour of DC grid voltages, currents and powers are shown in Fig 7. When the fault occurs, DC grid voltage collapses and high currents are generated discharging the capacitors of cable and converters. Once the arm currents of the converter are twice their rated value (2kA) or the DC voltage is less than $0.8p.u.$ a trigger is sent to block the MMC11 and MMC12 converter stations, to protect the MMC transistors. The faulty side (primary side) of the F2F-MMC converter also experiences over currents and to stop the DC fault from propagating to the healthy side, both sides MMC of the F2F-MMC converter are blocked. As a result, the DC power flow is stopped through the DC/DC converter and the faults are not propagated to the healthy side (DC grid 2). While fault current continues to be fed in DC grid 1 through AC grid.

Now, DC circuit breakers CB1 and CB3 are opened to isolate MMC11 station and the fault occurred on cable C11. A typical time of 10msec is considered for mechanical DC circuit breakers (DCCB) [11, 18]. After fault isolation, MMC12 and

F2F-MMC are unblocked to re-establish the power flow. As this time coordination is out of the scope of this paper, 30msec time interval is assumed for unblocking and re-energizing the cable C12.

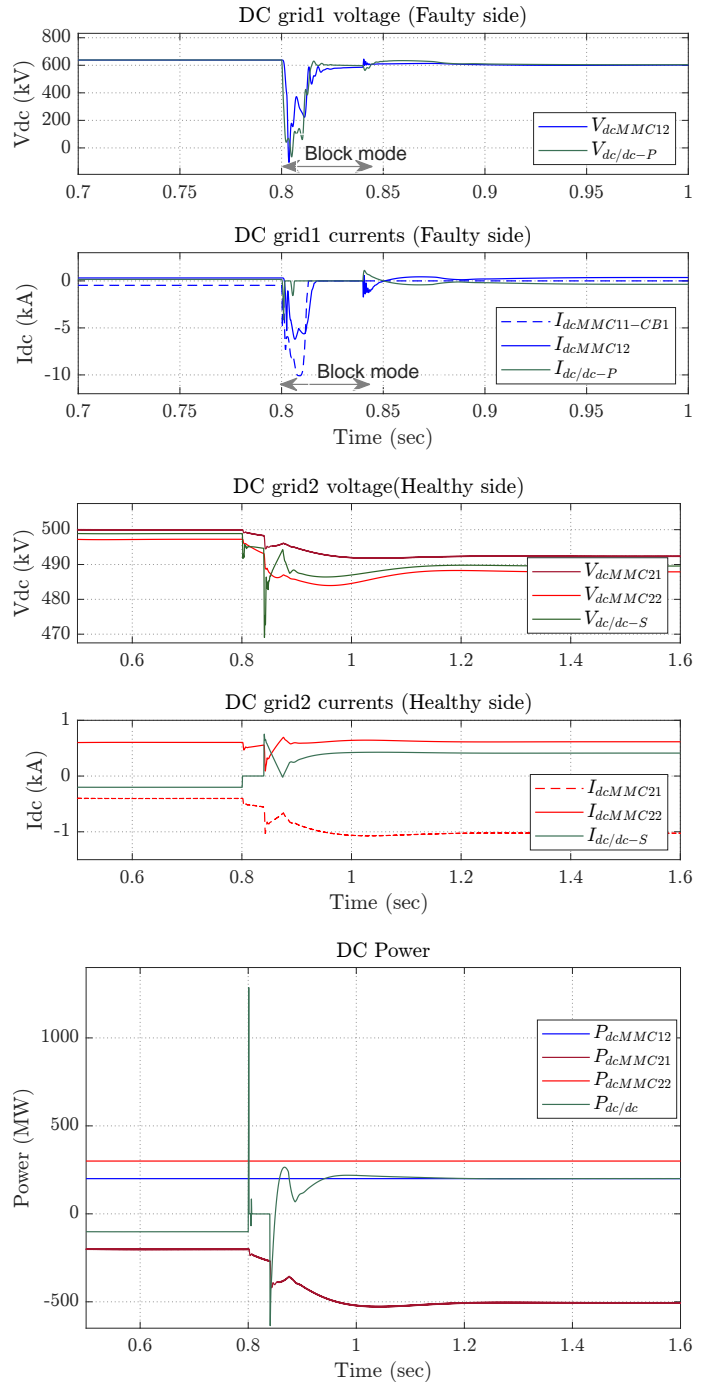


Fig. 7: Case 1: Pole to pole fault at DC grid1: Variation of DC powers, DC grid voltages and DC currents

In DC grid 1, after the isolation of the fault, there is no voltage controlled converter station to provide the power to the MMC12 station. So in a usual scenario, DC grid 1 will collapse. However, here the two DC grids are coupled and share

their power disturbances through the F2F-MMC virtual resistance controller. As a result, MMC21 (DC grid 2) provides the power to MMC12 station after the fault. So, as we can observe from Fig 7, the power flow can be re-established thanks to the virtual resistance controller. The healthy side (DC grid 2) experiences a voltage dip and transients on its power and current waveform, but still, the voltages are under the 5% limits.

4.2 Case 2: Pole-to-pole fault at DC grid2 with control of F2F-MMC

In this section, DC fault is applied near the voltage controlled station MMC21 at DC grid 2. Similar to the previous case, a pole-to-pole fault is applied at 0.8sec at the middle of the cable C21, 125km from station MMC21. In the previous case, the fault is stopped from propagating to the healthy side by blocking both sides MMC's of the F2F-MMC converter. This block mode is achieved from the non-controllable activation of diodes and results in an abrupt change in DC/DC converter power. Thus, to avoid activating the block mode of the F2F-MMC converter, in this case, a control approach of F2F-MMC is employed to stop the propagation of the DC fault to the healthy side [8].

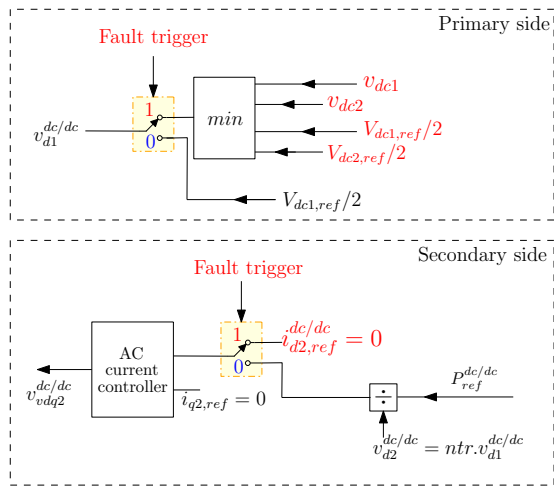


Fig. 8: F2F-MMC AC side fault control in dq frame

During the faulty mode, F2F-MMC is controlled as shown in Fig 8. The fault trigger is set to 1 when the DC voltage is less than $0.7p.u.$ and F2F-MMC goes into fault mode. The AC voltage output which is fixed by the primary side is decreased and controlled to follow the minimum value between the DC fault voltage which is near zero or to the value $\min[V_{dc1,ref}/2, V_{dc2,ref}/2]$ to avoid activating the block state. So, there is a very low AC voltage to supply the fault current. Also, in order to converge the power of the DC/DC converter to zero, the AC current which is controlled by the secondary side of F2F-MMC is set to zero when the converter goes into fault mode. Thus, there is no power flowing through the DC/DC converter and as a result, the fault is not propagated to the healthy side (DC grid 1).

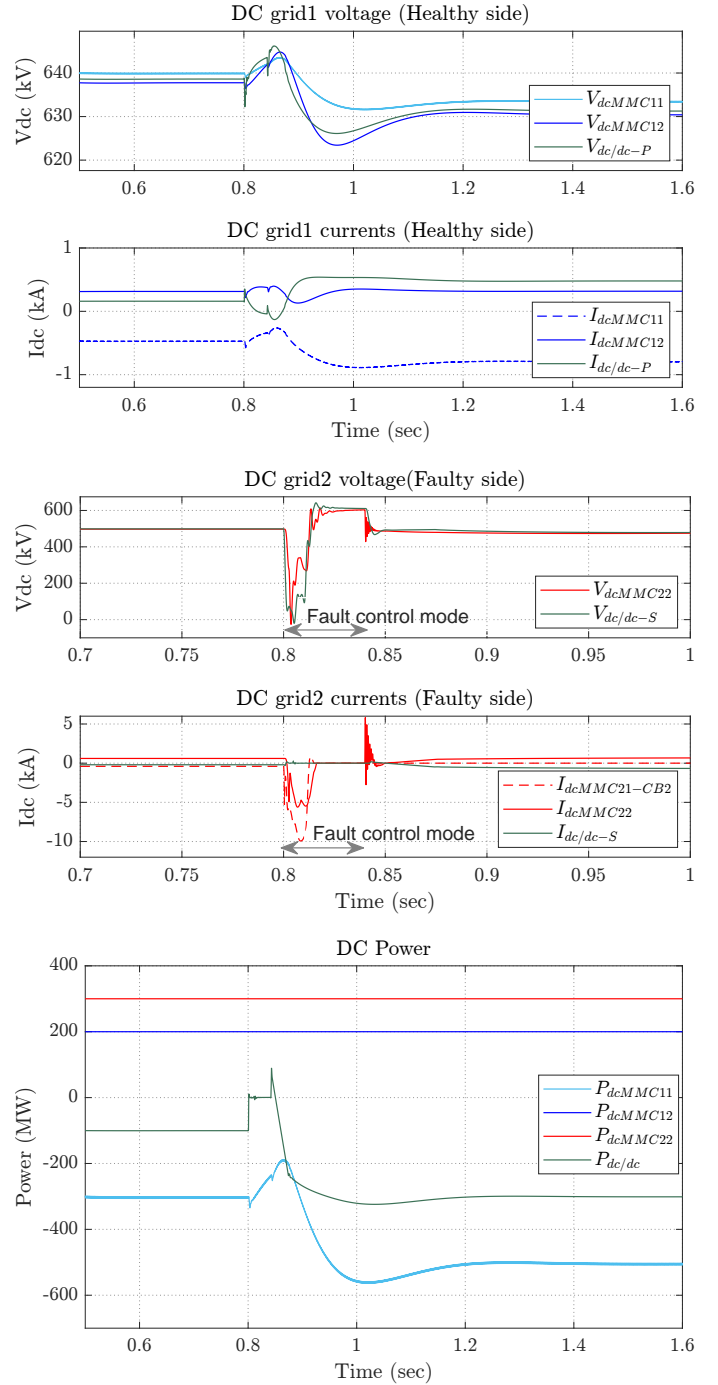


Fig. 9: Case 2: Pole to pole fault at DC grid2 with F2F-MMC fault control: Variation of DC powers, DC grid voltages and DC currents

The resulting DC voltage, currents and powers are presented in Fig 9. After 10msec circuit breakers CB2 and CB4 are opened, isolating the DC fault and station MMC21. MMC22 is unblocked and cable C22 is energized in assuming the time interval of 30msec similar to case 1. Once DC grid 2 voltage starts to reach within its acceptable limit of $\pm 5\%$ of nominal value, the fault trigger is set to 0 and the F2F-MMC control is shifted to its normal mode. As can be observed from Fig 9,

the DC/DC converter power does not have an abrupt transient, instead the power is controlled smoothly.

Hence, for this case also, the new power flow is re-established with the remaining system, where station MMC11 (DC grid1) shares the power of station MMC12 (DC grid 1) and MMC22 (DC grid2). By the action of the virtual resistance controller, MMC11 modified its power in order to compensate for the loss of MMC21 station after the DC fault and prevented the collapsing of DC grid 2.

Thus, with the help of virtual resistance control, we are able to re-establish the power flow and share the power disturbances between the interconnected DC grids after the isolation of DC faults. Therefore, through the virtual resistance controller, the power flow is restored in critical cases of DC faults and this lowers the risk of collapsing of the faulty grids. This highlights the added advantage of the virtual resistance DC voltage controller with the DC/DC converter.

5 Conclusion

DC/DC converters have the ability to provide several functionalities in the development of future MTDC networks. They are an obligatory component in interconnecting grids of different specifications. F2F-MMC converter can provide protection during DC faults by acting as a firewall between the healthy and faulty sides. Along with this, DC/DC converter integrated with a DC voltage controller can establish a link between the interconnected grids and can help in DC voltage management. An EMT study has been presented with the DC/DC converter interconnecting two P2P links with different voltage levels, where the DC/DC converter works in voltage control mode with the virtual resistance voltage controller. The system is applied with a critical case of pole-to-pole DC faults at both grids in different cases. The impact of F2F-MMC with virtual resistance DC voltage controller is analysed in the restoration of the system. It has been observed that the DC/DC converter with the virtual resistance controller can help in re-establishing the power flow of the remaining system after the isolation of DC fault. As illustrated, thanks to the virtual resistance DC voltage controller, the system is able to restore its power flow even in the critical case of a DC fault. This reduces the risk of collapsing faulty grids. Therefore, the virtual resistance DC voltage controller associated with the DC/DC converter has an added advantage in HVDC system restoration in case of faulty conditions. Further analysis could be done with other DC/DC converter topology and grounding configurations of the system.

6 Acknowledgements

This work was developed during the DICIT project sponsored by a public grant overseen by the French National Research Agency as part of the “Appel à Projet Générique” (ANR-20-CE05-0034 DICIT).

7 References

- [1] Buigues, G., Valverde, V., Etxegarai, A., Eguía, P., Torres, E.: ‘Present and future multiterminal HVDC systems: current status and forthcoming’, *Renewable Energy and Power Quality Journal*, 2017, 1, (15), pp. 83–88
- [2] ‘Friends of Sustainable Grids | Interconnecting Electricity for Europe’s Sustainable Future’, <https://supergrid.brussels/>, accessed 1 February 2024
- [3] Kolparambath, S.K., Suul, J.A., Tedeschi, E.: ‘DC/DC converters for interconnecting independent HVDC systems into multiterminal DC grids’. *IEEE 13th Brazilian Power Electronics Conference and 1st Southern Power Electronics Conference (COBEP/SPEC)*, Fortaleza, Brazil: IEEE, Nov. 2015, pp. 1–6
- [4] Dworakowski, P., Gomez.A., D., Paez, J.D., Cheah.Mane, M., Maneiro, J., Gomis.Bellmunt, O., et al.: ‘Requirements for interconnection of HVDC links with DC-DC converters’. *IECON 2019 - 45th Annual Conference of the IEEE Industrial Electronics Society*, Lisbon, Portugal: IEEE, Oct. 2019, pp. 4854–4860
- [5] CIGRE WG. B4. 76., ‘DC-DC converters in HVDC grids and for connections to HVDC systems’, 2021, <https://e-cigre.org/publication>
- [6] Dworakowski, P., Paez, J.D., Frey, D., Maneiro, J., Bacha, S.: ‘Overview of DC–DC Converters Dedicated to HVdc Grids’, *IEEE Transactions on Power Delivery*, 2019, 34, (1), pp. 119–128
- [7] Adam, G.P., Gowaid, I.A., Finney, S.J., Holliday, D., Williams, B.W.: ‘Review of dc–dc converters for multiterminal HVDC transmission networks’, *IET Power Electronics*, 2016, 9, (2), pp. 281–296
- [8] Gruson, F., Tlemcani, A., Li, Y., Delarue, P., Le.Moigne, P., Guillaud, X.: ‘Model and control of the DC–DC modular multilevel converter with DC fault tolerance’, *EPE Journal*, 2020, 30, (4), pp. 153–164
- [9] Gowaid, I.A., Adam, G.P., Massoud, A.M., Ahmed, S., Holliday, D., Williams, B.W.: ‘Quasi Two-Level Operation of Modular Multilevel Converter for Use in a High-Power DC Transformer With DC Fault Isolation Capability’, *IEEE Transactions on Power Electronics*, 2015, 30, (1), pp. 108–123
- [10] Páez, J.D., Maneiro, J., Frey, D., Bacha, S., Bertinato, A., Dworakowski, P.: ‘Study of the impact of DC-DC converters on the protection strategy of HVDC grids’. *15th IET International Conference on AC and DC Power Transmission (ACDC 2019)*, Coventry, UK: Institution of Engineering and Technology, 2019, pp. 29 (6 pp.)–29 (6 pp.)
- [11] Li, R., Xu, L., Yao, L., Williams, B.W.: ‘Active Control of DC Fault Currents in DC Solid-State Transformers During Ride-Through Operation of Multi-Terminal HVDC Systems’, *IEEE Transactions on Energy Conversion*, 2016, 31, (4), pp. 1336–1346
- [12] Sun, K., Li, K.J., Wang, M., Tian, G., di Wang, Z., Liu, Z.: ‘Coordination control for multi-voltage-level dc grid based on the dc–dc converters’, *Electric Power Systems Research*, 2020, 178, pp. 106050
- [13] Beerten, J., D’Arco, S., Suul, J.A.: ‘Frequency-dependent cable modelling for small-signal stability analysis of VSC-HVDC systems’, *IET Generation, Transmission*

and Distribution, 2016, 10, (6), pp. 1370–1381

- [14] Paez, J.D. ‘DC-DC converters for the interconnection of HVDC grids’. PhD thesis, Communauté Université Grenoble Alpes, 2019
- [15] Zhang, H., Jovicic, D., Lin, W., Far, A.J.: ‘Average value MMC model with accurate blocked state and cell charging/discharging dynamics’. 4th International Symposium on Environmental Friendly Energies and Applications (EFEA), Belgrade, Serbia: IEEE, Sep. 2016, pp. 1–6
- [16] Samimi, S., Gruson, F., Delarue, P., Guillaud, X., ‘Synthesis of different types of energy based controllers for a Modular Multilevel Converter integrated in an HVDC link’. 11th IET International Conference on AC and DC Power Transmission, Birmingham, UK, Feb. 2015
- [17] Shinoda, K., Freytes, J., Benchaib, A., Dai, J., Saad, H., Guillaud, X.: ‘Energy difference controllers for mmc without dc current perturbations’. 2nd International Conference on HVDC (HVDC2016), Shanghai, 2016
- [18] Ito, H., Yamamoto, R., Kamei, K., Kono, Y., El.Oukaili, S., Yoshida, D., et al.: ‘HVDC circuit breakers for HVDC grid applications’. 11th IET International Conference on AC and DC Power Transmission, Birmingham, UK: Institution of Engineering and Technology, 2015, pp. 044 (9 .)–044 (9 .)